



Thermokinetic Study by Solar Convective Drying of Argan Press-Cake

Raja Idlimam^{1*}, Khaoula Chatir², Mohamed Asbik¹, Abdellah Bah¹, Haytem Moussaoui²

¹Thermal and Energy Research Team (ERTE), ENSAM, Mohammed V University in Rabat, Rabat 10100, Morocco

²Team of Solar Energy and Medicinal Plants EESPAM, Laboratory of Processes for Energy & Environment ProcEDE, ENS, Cadi Ayyad University, Marrakech 40000, Morocco

Corresponding Author Email: raja.idlimam@um5s.net.ma

<https://doi.org/10.18280/ijht.400121>

ABSTRACT

Received: 29 September 2021

Accepted: 14 January 2022

Keywords:

argan press-cake, convective drying kinetics, solar drying, characteristic drying law, activation energy

The argan tree "Argania spinosa" is a typically multi-use tree. It represents the agroforestry systems pivot which has so far succeeded in meeting the needs of the inhabitants of arid and semi-arid areas strongly marked by climatic hazards. Argan press-cake, residue from the argan oil extraction, is used in several fields, namely: cosmetics, agriculture, and pharmacology. In order to keep this argan paste with a pennyworth, solar drying is an economically appropriate solution, energy and environmentally friendly. In this work, an experimental study is performed to improve the sun-drying process of Argan press-cake using an indirect forced convection solar dryer. As a result, the evolution of the temperature and the drying kinetics inside the product have been assessed. The influence of air recycling drying on the drying time has been highlighted and the characteristic drying law was established too. Thus, the optimal storing conditions of argan press-cake were identified.

1. INTRODUCTION

Biomass is the whole of organic materials, mainly vegetable origin, natural or cultivated, terrestrial or marine, resulting from the chlorophyllic conversion of the solar energy. Energy conversion of biomass could be done according to three main processes: biochemical conversion (digestion, hydrolysis and fermentation); chemical conversion (esterification); and thermochemical conversion: combustion, co-combustion, pyrolysis and gasification [1-6].

The argan tree (*Argania spinosa* (L.) Skeel, belongs to the Sapotaceae family and is the only species of this family of tropical plants found in subtropical areas. The genus *Argania* is the only species endemic to Morocco: *Argania spinosa* (syn. *Argania syderoxydon* L., *Sideroxydon spinosum* L. *Elaeandronargan* Retz) [7]. Etymologically, the word Argan (the tree) comes from the Berber word arjān, which derives from rajnah which means in Berber dialect (to remain closed) in a limited space. In fact, the argan tree is endemic to Morocco, mainly located in the arid and semi-arid areas of southwest Morocco along the oceanic coast, from the mouth of the Wadi Tensift in the north to the mouth of the Wadi Drāa in the south, where it covers an area of 828 000 ha [8]. The argan tree also grows in the plain of Souss, on the southern slopes of the Western High Atlas and on the northern and southern slopes of the Western Anti-Atlas up to altitudes of 1300-1500 m [9], and it fruits abundantly when it is not grazed by goats, or attacked by Ceratitis (fruit fly). It is a wild species, hardly domesticated.

This tree is in the heart of social and economic life for more than 3 million people, including 2.2 million in rural areas. It represents a valuable resource for the economy and the environment. The argan tree is typically multi-purpose, it represents the pivot of agro-forestry systems that have succeeded so far to meet the needs of the inhabitants of these

areas strongly marked by climatic hazards [10]. The disappearance of the argan tree inevitably leads to the disappearance of many animal and plant species. The argan tree is traditionally inhabited by the Amazigh population, who has developed through the ages, a particular way of life centered on the argan tree. It has allowed the creation of several jobs through the creation of cooperatives and especially women who practice a tedious and manual work to extract the argan oil and recover the argan press-cake, which is one of the waste products [11]. These women have an ancestral know-how that has been transmitted from mother to daughter in order to preserve this tradition and enhance their local products. In addition, traditional knowledge mentions two main varieties: one with a thin shell that is easily broken by hand but the other is broken with greater difficulty, producing a mesocarp that dries in one piece and is harvested and stored for the herds during the dry season.

The three main products of the argan tree are:

- Argan oil extracted from the almond (spills in a hull or endocarp);
- the press-cake resulting from the oil by pressure;
- the mesocarp or pulp consumed dromedaries and goats;
- young leaves eaten by dromedaries and goats.

The argan press-cake or the residue of the extraction of argan oil is currently used as feed for cattle submitted to fattening. It is rich in carbohydrates, protein ranging from 23 to 41% [12] and contains an important pharmacodynamic group consisting of saponins [13]. It has antiviral, antifungal, analgesic, anti-tumor and other actions but above all it stimulates the biosynthesis of glutathione produced by human fibroblasts [14, 15]. It also has remarkable biological properties that favor its use in the field of cosmetology, notably, an excellent anti-wrinkle and a very good anti-acne. It could be used as a natural soap as it is, for its washing,

scrubbing action without forgetting the emollient action since it also contains the residual oil that has a moisturizing and antioxidant power compensating for the denutrition of the skin.

The argan press-cake represents a relatively new international product, exported only by Morocco. The growing demand of consumers and foreign distributors of argan press-cake will lead to increase its export in the future in significant quantities on foreign markets worldwide. Hence the need to seek a solution to preserve it to ensure continuity in its availability and meet demand in terms of a good value for money and allow transport at lower cost. Several solutions are proposed: cultivation in greenhouses, freezing, conservation by drying. Solar drying with forced convection as a method of valorization is one of the effective, sure and adequate thermal processes for the conservation of agro-alimentary product.

Morocco has considerable solar potential with a sunshine of 3 000 hours per year and an average irradiation of more than 5 kWh.m⁻², a growing interest was shown in favor of solar drying. Indeed, this conservation technique, economical in energy, is likely to extend the period of availability of products, so to confer them appreciated physicochemical properties. It is the process of elimination of moisture in the product up to a certain threshold value by evaporation. Therefore, the product can be stored for a long time [16, 17]. In this respect, drying is considered the best process for removing water and solvents from wet solids. Products are often poorly dried and invaded by pests. Solar drying provides heat to the product and reduce its humidity by keeping it in clean conditions. It improves its quality and protects the environment [18].

This work focuses on a thermokinetic study by solar convective drying of argan press-cake. In this study, we are interested in the experimental macroscopic approach, which consists of determining the kinetic behavior of the argan press-cake during its drying under controlled temperature and air flow conditions using a partial solar indirect dryer in thin layer and forced convection. The different experimental tests concern the separate influence of the various conditions of the drying air (temperature and air flow) on the drying process. The drying rate is empirically determined from the characteristic curve of drying (CCD). The obtained experimental drying curves are mathematically modeled to establish a law of drying characteristic of argan cake and hence estimate the diffusion coefficient and the activation energy.

2. MATERIALS AND METHODS

2.1 Description of the solar drying system

The experimental device is an indirect dryer coupled with a convective solar collector (Figure 1). The system operates without storage and with total or partial recycling of air [19, 20]. It is composed of the following elements:

- A single-circulation, single-glazed solar collector, inclined at 31° to the horizontal plane and facing due south. The collector has a surface area of 2.5 m². The cover is made in ordinary glass. The absorber of the solar collector is made of a blackened galvanized iron sheet with a non-selective surface. The rear thermal insulation is made of polyurethane foam sandwiched between two steel sheets.
- An aeraulic suction pipe consisting of a tunnel with a parallelepiped section. A double T (consisting of two nested T) allows the total or partial recirculation of the

air leaving the drying chamber after crossing all the racks.

- A drying chamber consisting of ten trays.
- A centrifugal ventilator (0.0889 m³/s; 80 mm CE, 220V), allows a theoretical speed of 1.7 m/s, with a throttle upstream that allows the air flow to vary from 0.0296 to 0.0889 m³/s. This ventilator has a power of 0.1 kW.
- A thermoregulator with a range of 0-99°C and a precision of 0.1°C connected to a PT100 platinum probe acting on the electric auxiliary heating allows to fix the set temperature at the entrance of the drying chamber.
- Electric resistances of power 4 kW playing the role of an auxiliary source of energy.

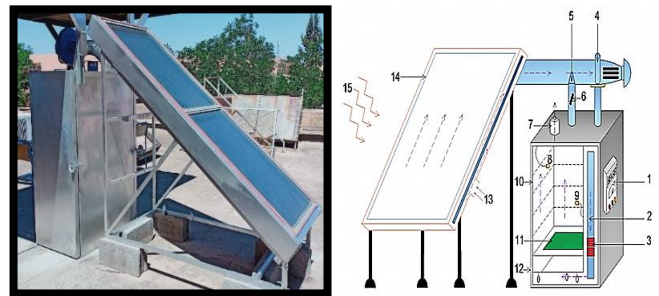


Figure 1. Convective solar dryer installed in Marrakech (1) control box, (2) suction pipe, (3) electrical backup, (4) ventilator, (5) ventilation pipe, (6) air flap, (7) air outlet, (8) humidity sensor, (9) thermocouple, (10) floors, (11) sample door, (12) drying cabinet, (13) air inlet, (14) solar sensor, (15) solar radiation

The instruments used in the drying experiments are shown in Figure 2:



Figure 2. Instruments used in the drying experiments

2.2 Sampling and experimental procedure

2.2.1 Preparation of samples

With the purpose of determining the characteristic curves of drying, the dryer was used by setting the conditions of air inlet.

Firstly, we kneaded the argan paste with a roller to form it into pieces in the form of small tiles of equal mass 20 g, a thickness equal to 4 mm and a length of 1.5cm. The prepared samples (Figure 3) are then weighed and distributed evenly and regularly on porous sample holders, so that we can ensure that the samples of argan cake receive a uniform heated air during the drying process.

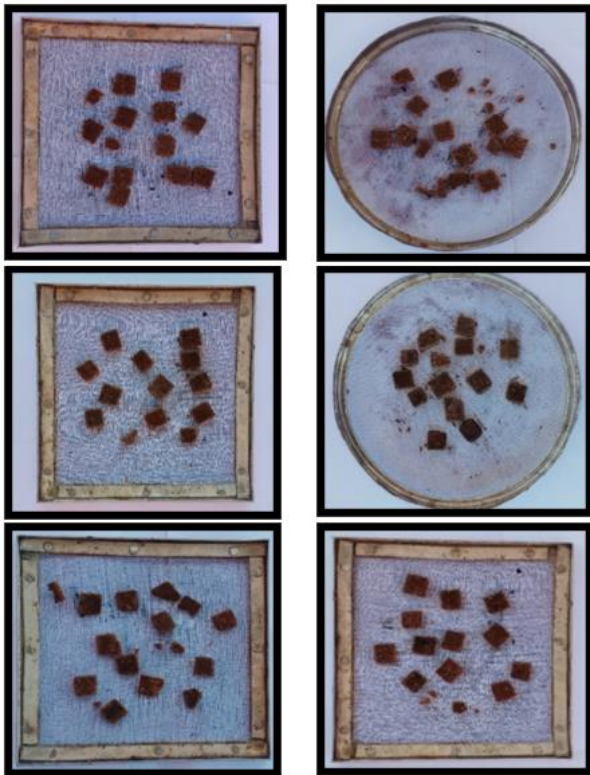


Figure 3. Samples of argan press-cake before the drying process

2.2.2 Experimental protocol

In order to ensure a better stability of the drying conditions and a homogenization of the temperature inside the dryer, the whole equipment must be operated at least half an hour before the introduction of the loaded racks in the drying chamber.

The variation of the wet mass of the product as a function of time is determined by static weighings of 30 s duration, by means of a balance of precision ± 0.1 g. The time step varies from 10 min. As soon as the mass reaches an equilibrium value, the drying time is calculated. The measurement at time t gives us the wet mass of the product $M_h(t)$. The drying experiment is stopped when three successive weighings show a difference not exceeding 0.01.

2.3 Drying characteristic curve (DCC)

The identification of the qualifying curve of drying consists of representing the kinetics of drying by an empirical equation acquired by the adjustment of the realized experimental curves. This identification tends to couple the experimental results obtained on a product concerning several conditions of the drying air on a single basic curve called characteristic curve of

drying (DCC). Thus, drying curves personify either the curves that tune the drying rate as a function of time t and water content X , or those that represent the variations of water content X as a function of time t , or a reduced form of the latter that aims to provide a single representation for various drying conditions. Many authors [21-23] have exploited the concept of characteristic curves in order to determine the expression of the drying rate of a product.

The approach was stated and developed, in 1958, by Van Meel [24]. The DCC archetype can only be adopted for thin film samples and allows to neglect the diffusion gradients as well as the non-massive ones. Some authors have exploited the notion (DCC) in order to specify the expression of the drying rate of a product. The experimental calculations allow to acquire a set of drying curves.

The drying characteristic curve (DCC) describes the drying rate at time t $(-\frac{dX}{dt})_t$ compared to the drying speed in the first step $(-\frac{dX}{dt})_I$, according to the reduced water content $\frac{X-X_{eq}}{X_{cr}-X_{eq}}$. The general form of the equation of the drying characteristic curve is given by: $f = f(X^*)$.

In the case where the product has phase I, the determination of $(-\frac{dX}{dt})_I$ is quite simple, it corresponds indeed to the speed of the phase at constant rate. However, in the case of drying food products, the first phase is usually absent, which implies that: $(-\frac{dX}{dt})_I = (-\frac{dX}{dt})_0$ and $X_{cr} = X_0$ [25].

$$\text{X-axis: } X^* = \frac{X(t) - X_{eq}}{X_{cr} - X_{eq}} = \frac{X(t) - X_{eq}}{X_0 - X_{eq}} \quad (1)$$

$$\text{Ordinate: } f = \frac{(-\frac{dX}{dt})_t}{(-\frac{dX}{dt})_I} = \frac{(-\frac{dX}{dt})_t}{(-\frac{dX}{dt})_0} \quad (2)$$

where

X^* is the reduced water content;

f represents the normalized drying rate;

$X(t)$ is the instantaneous water content (kg water/kg MS);

X_{cr} refers to the critical water content (kg water/kg MS);

X_0 designates the initial water content (kg water/kg MS);

$(-\frac{dX}{dt})_t$ is the drying rate at time t (kg water/kg MS. min);

$(-\frac{dX}{dt})_I$ is the drying rate of phase I (kg water/kg MS. min);

$(-\frac{dX}{dt})_0$ is the initial drying rate (kg water/kg MS. min).

The function $f = f(X^*)$ verifies the properties presented by the system of Eq. (3) for a set of experimental points under different constant experimental conditions during drying (temperature, air flow rate, air humidity, and product dimensions).

$$\begin{cases} f = 0 \text{ for } X^* = 0 \\ 0 \leq f \leq 1 \text{ for } 0 \leq X^* \leq 1 \\ f = 1 \text{ for } X^* \geq 1 \end{cases} \quad (3)$$

Although the validity of this model can be shown theoretically, it should rather be considered as an experimental attempt to present a set of results in a particularly simple form that can be used under a range of experimental conditions for which the predominant physical mechanisms remain the same.

2.4 Diffusion coefficient

Diffusion is mechanism involving the microscopic mass

transport of moisture to the product surface where it could be evaporated. The effective diffusivity of moisture is generally obtained from the slope of $\ln(X^*)$ versus time. The Fick diffusion equation [26, 27] is applied to experimental results. The following equation describes the analytical solution of Fick's second law:

$$\ln(X^*) = \ln\left(\frac{8}{\pi^2}\right) - \left(\frac{\pi^2 D_{eff}}{4L^2}\right) \times t \quad (4)$$

D_{eff} and L are the effective diffusivity coefficient (m^2/s) and the half thickness of the product (m), respectively.

The diffusion coefficient for each drying temperature was calculated by substituting the experimental data into the previous equation. The diffusion coefficient is determined by plotting the experimental drying data in terms of $\ln(X^*)$ versus drying time. Plotting Eq. (4) results in a straight line with slope:

$$K = \left(\frac{\pi^2 D_{eff}}{4L^2}\right) \quad (5)$$

2.5 Activation energy

The concept of activation energy appeared at the end of the 19th century. It corresponds to the quantity of energy that must be supplied to a system to initiate a chemical reaction. It is represented by E_a and appears in the Arrhenius' law giving the effective diffusivity [28, 29]:

$$D_{eff} = D_0 \times e^{\left(\frac{-E_a}{RT}\right)} \quad (6)$$

This formula is a function of the pre-exponential factor D_0 (m^2/s); the activation energy E_a ($kJ.mol^{-1}$); the drying temperature T (K) and the perfect gas constant R ($kJ.mol^{-1} K^{-1}$).

The activation energy was estimated by representing the natural logarithm of the experimental values of the effective diffusivity D_{eff} as a function of the inverse of the temperature, thus Eq. (6) is transformed into the form:

$$\ln(D_{eff}) = \ln(D_0) - \frac{E_a}{R} \left(\frac{1}{T}\right) \quad (7)$$

3. RESULTS AND DISCUSSION

The drying experiments were carrying out during the month of May 2021 for the argan press-cake within the Solar Energy and Aromatic and Medicinal Plants Team of the Ecole

Normale Supérieure, Cadi Ayyad University, Marrakech, Morocco. Climatic conditions (ambient air temperature, solar radiation and relative humidity) for this period are depicted on Figure 4a-b. Indeed, the temperature of the ambient air and the ambient relative humidity were ranging from 15 to 38°C, and 11 to 46%, respectively.

Experimental measurements were performed for three drying air temperatures (40, 50, and 60°C \pm 0.3°C) and for two air flow rates (150 and 300 \pm 2 m³/h). Table 1 gives the drying conditions for the different tests.

Figure 5 represents the photos of Argan press-cake after the drying process using the solar dryer by forced convection with temperatures 40°C, 50°C, and 60°C, and for two air flows 300 and 150 m³/h. A change of color is noticed, which proves degradation of the pigments of the press-cake during the solar drying process.

Figure 6 shows the samples of Argan cake after solar drying for three temperatures 40, 50 and 60°C. From this figure we see that there is a change in color from dark brown to light brown while increasing the temperature of treatment. This fact shows that the temperature has significant impact on the pigments of Argan press-cake.

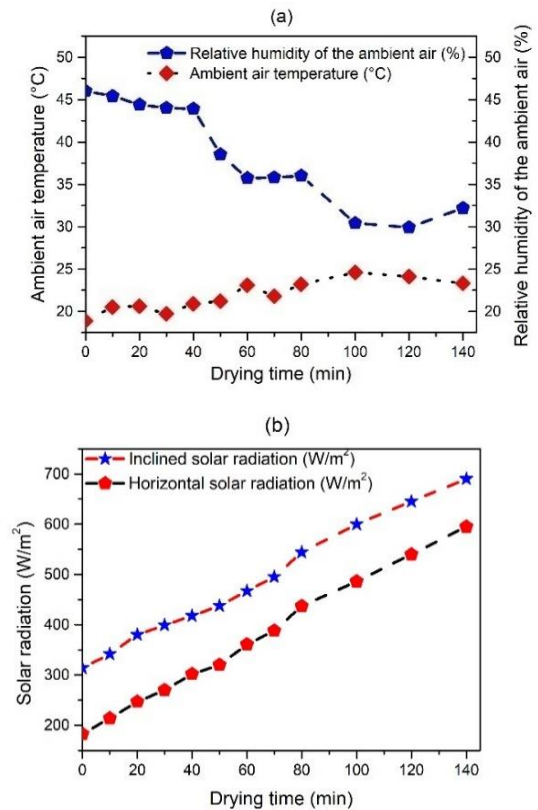


Figure 4. Variation of ambient relative humidity, ambient air temperature and solar radiation during the 50°C drying temperature experiment

Table 1. Drying conditions for the different tests

Experiments	Db \pm 2 (m ³ .h ⁻¹)	T \pm 0.3 (°C)	X ₀ \pm 0.001 (kg water/kgMs)	X _t \pm 0.001 (kg water/kgMs)	Time (min)
1	300	40	0.30	0.12	290
2	300	50	0.30	0.09	230
3	300	60	0.26	0.06	210
4	150	40	0.34	0.13	430
5	150	50	0.31	0.11	260
6	150	60	0.31	0.09	230

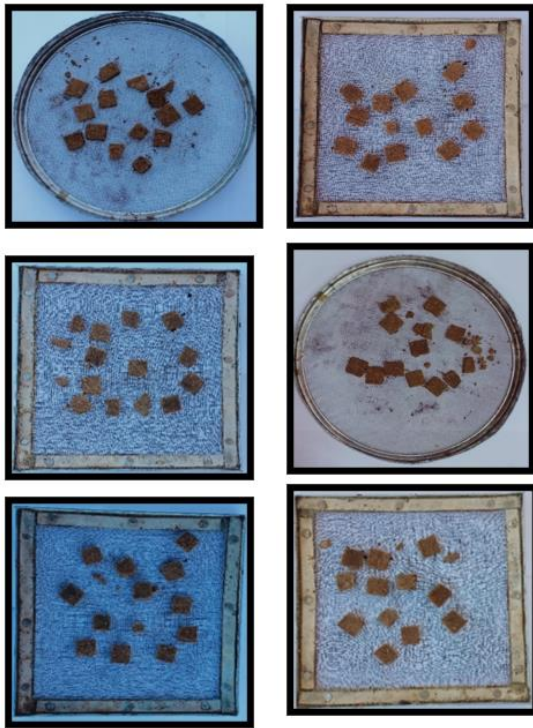


Figure 5. Samples of Argan press-cake after the drying process

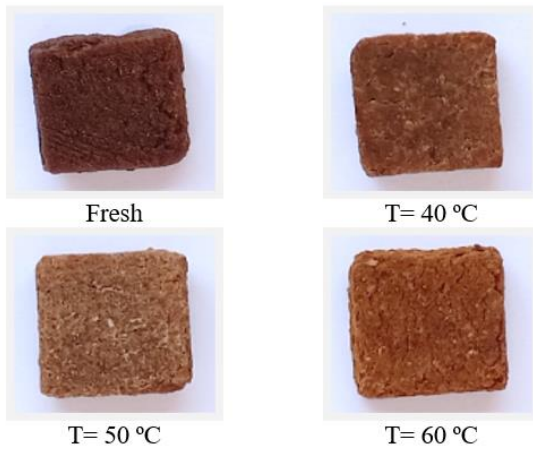
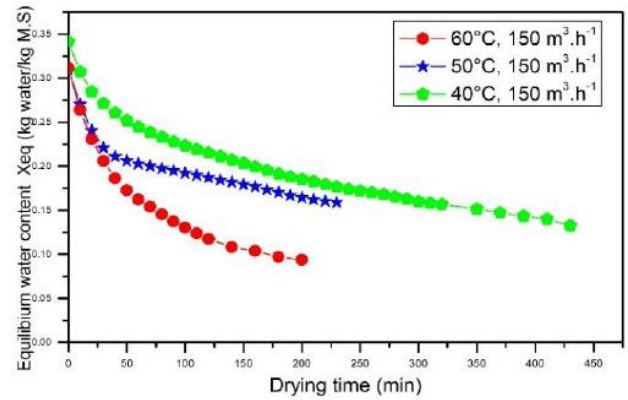


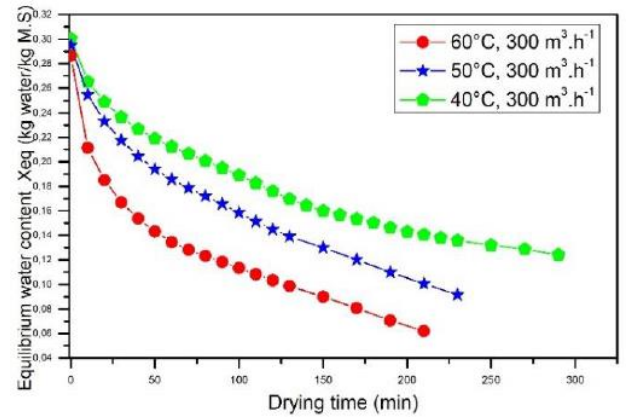
Figure 6. Samples of Argan press-cake after the drying process with the presence of a change in color

3.1 Solar drying kinetics

Figure 7a-b exhibits the evolution of water content versus drying time for two different drying air conditions (150 and 300 m³/h) and at three temperatures (40, 50 and 60°C). These figures highlight the influence of temperature and drying air rate on the equilibrium moisture content and drying time. It is obvious that these last quantities decrease over time and the increase of drying air rate accelerates the drying process and reduces the residence for product in the solar dryer. In the same conditions of temperature and drying air, the behavior of the drying rate as a function of the water content is shown in Figure 8a-b whose curves show a decreasing trend of the reduced water content as a function of the drying time. They lay out very clearly, for both flow rates, the absence of two drying periods (or phases) namely, phase 0 (initial phase) and phase 1 (constant rate phase). These results are in good agreement with the literature [1, 5, 30-33].

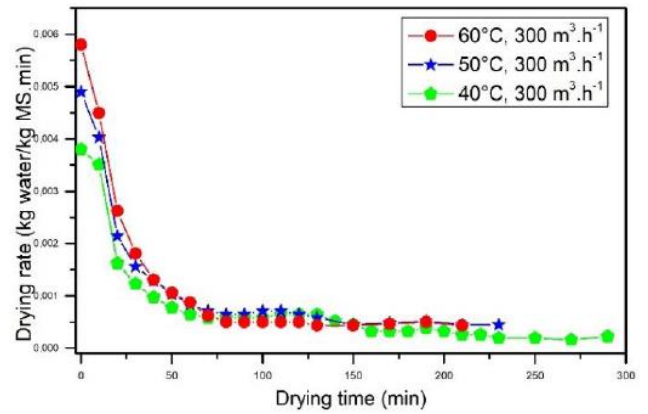


(a)

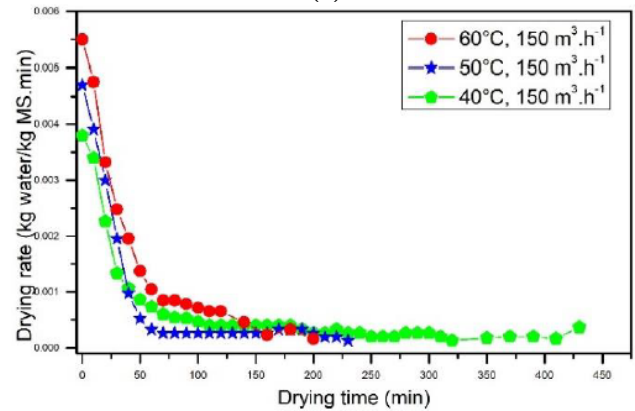


(b)

Figure 7. Temporal evolution of the water content of Argan press-cake



(a)



(b)

Figure 8. Evolution of the drying rate of Argan press-cake versus time

The variation of the drying rate with respect to the water content at different conditions of solar convective drying is shown in Figure 9a-b. As expected, the drying rate of Argan cake increases with the aforementioned parameters, and the impact of temperature on the drying rate is significantly higher than that of drying air flow rate. Moreover, the residence time in the dryer increases with a decreasing the temperature of the drying air. Therefore, a higher drying temperature produced a higher drying rate. These results are similar to those of the literature based on solar drying of food products [28, 34-37].

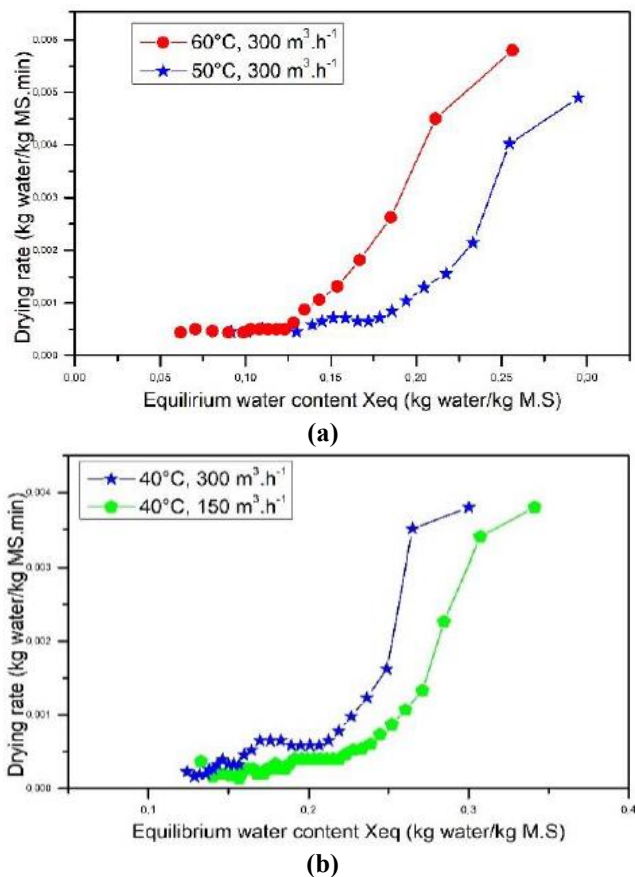


Figure 9. Impact of aerothermal parameters on the drying rate of Argan cake

3.2 Drying characteristic curve

This curve has a great interest since it is sufficient to know the values of the initial and equilibrium absolute humidity allowing the description of the drying kinetics in any condition of the drying air. The principle of the drying characteristic curve is to reduce the set of experimental data in such a way that they can be put into a form that can be used not only by the experimenter himself, but also by the whole scientific community [25]. The process adopted consists in studying the evolution of the normalized drying rate as a function of the reduced water content X^* . This leads to a grouping of the different values (Figure 10) obtained around a single average curve which is the drying characteristic curve (DCC). Consequently, the equation representing the kinetics of drying of the product is written as $f = f(X^*)$. It gives a good approximation of drying curves despite the variations of aerothermal properties of the air.

The smoothing of the characteristic curve of drying of Argan cake has been determined as a polynomial of degree 4:

$$f = 3,095X^* - 2,786X^{*2} - 2,178X^{*3} + 2,912X^{*4} \quad (8)$$

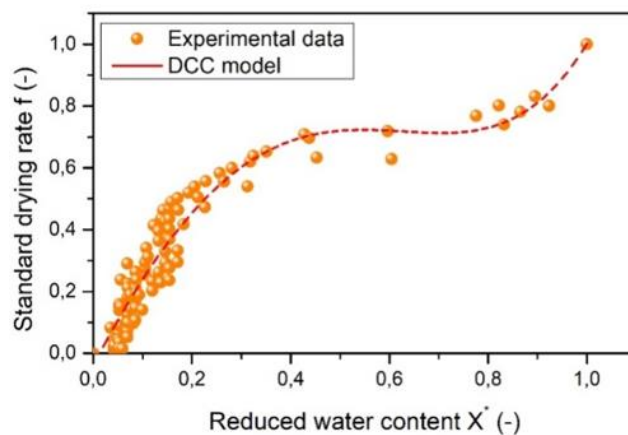


Figure 10. Characteristic curve of drying rate of Argan press-cake

The criteria used to predict the best equation that represents the drying characteristic curve are the correlation coefficient $r^2=0.9523$, the fit coefficient $r^2_{adj}=0.96$ and the standard error $SEE=0.3642$. Figure 11 shows the residual of the data predicted by the model of the drying characteristic curve, we notice that residuals vary between -2 and +2 for all experimental points.

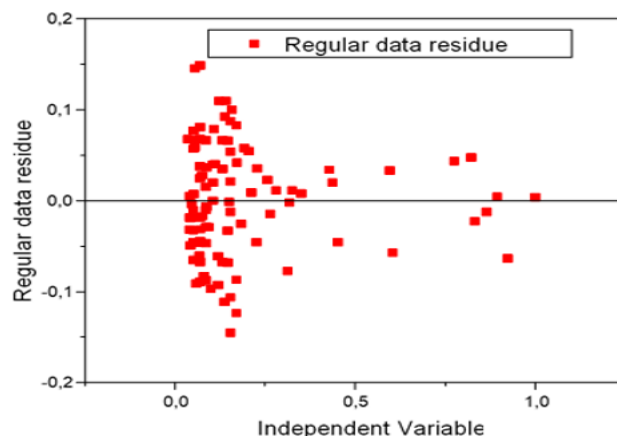


Figure 11. Predicted data residue by the drying characteristic curve model

3.3 Diffusion coefficient and activation energy

3.3.1 Diffusion coefficient

Figure 12a-b presents curves of $\ln(X^*)$ as a function of drying time for different temperatures and air flow rates. These curves clarify the influence of the drying temperature on the effective diffusion coefficient of water in Argan press-cake. We observe from these figures (12a and 12b) that the mass transfer increases with the temperature of the drying air.

As exposed in Table 2, it can be seen that the diffusion coefficient increases with increasing temperature and air flow rate respectively. Thus, the diffusivity varies from 1.79×10^{-8} to 3.41×10^{-8} (m^2/s) for convective drying of Argan cake in different aerothermal conditions. The values of D_{eff} are generally ranging within the interval of those of food products ($10^{-11} < D_{eff} < 10^{-9}$) [23, 38].

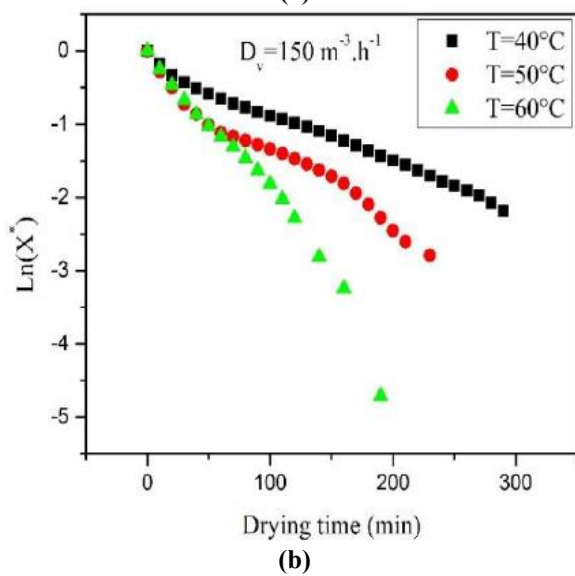
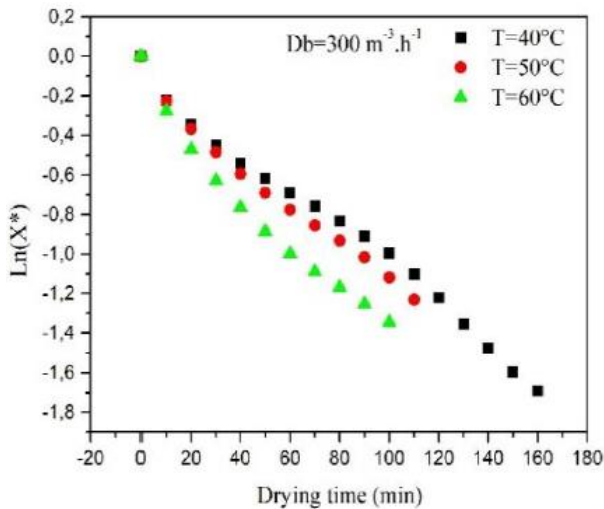


Figure 12. Influence of the drying temperature on the effective diffusion coefficient of argan press-cake

Table 2. D_{eff} values of Argan press-cake for different arothermal parameters

T (°C)		40	50	60
D_{eff} (m ² /s)	$D_v=300\text{m}^3/\text{h}$	$1,94 \cdot 10^{-08}$	$2,48 \cdot 10^{-08}$	$3,41 \cdot 10^{-08}$
	R^2	0,95	0,97	0,96
$D_v=150\text{m}^3/\text{h}$	R^2	0,96	0,96	0,97

3.3.2 Activation energy

Activation energy is the minimum quantity of energy needed to activate drying kinetics allowing water molecules to diffuse. It gives the required energy allowing water molecules to start the self-diffusion, which is provoked by thermal energy. To estimate this main parameter, a graph of experimental points is plotted on Figure 13a-b for each air flow rate (150 and 300 m³/h). As a result, $\text{Ln}(D_{eff})$ is a linear function of $1/T$ which proves that these results verify the Arrhenius Law and hence the activation energy deduced from them is 10.81 kJ/kg.

In this context, it is found that the activation energy is more sensitive to the variation of temperature than that of air flow rate. This could be explained by the high amount of heat brought to the product compared to the kinetic energy of air which provokes saturation pressure variations. The values

found are comparable to those found in the literature obtained with other drying techniques and for other dehydrated food products [39-41].

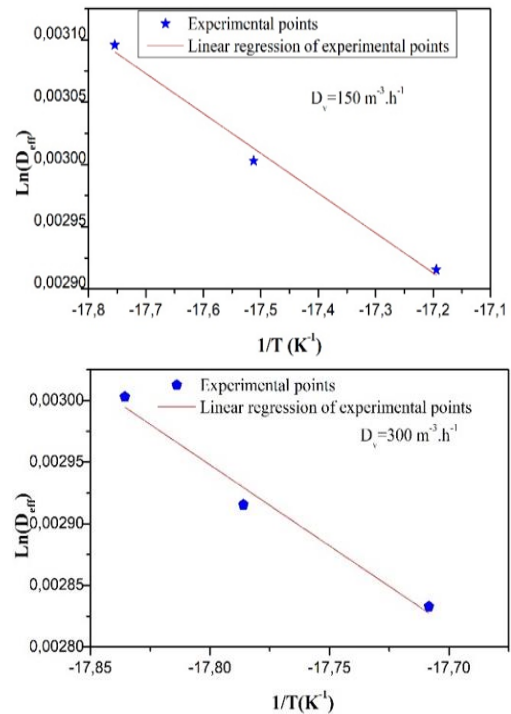


Figure 13. $\text{Ln}(D_{eff})$ versus $1/T_{abs}$ for three temperatures and two drying air flows

4. CONCLUSION

In this work, the experimental study of solar drying with forced convection of Argan press-cake was conducted for a configuration of three temperatures (40, 50 and 60°C) and for two air drying flow rates (150 and 300 m³.h⁻¹). It has been shown that drying kinetics depends strongly on those parameters (temperature and flow rate) and their associated curves have decreasing trend. Thus, as for most food products, it was noticed the absence of phase 0 (initial phase) and phase I (constant rate phase) contrary to the phase II (with decreasing rate). The analysis of the hygroscopic balance of the Argan cake shows that their behavior is directly affected by the flow of drying air and for the set temperature. In addition, the drying temperature is the main factor that affects the drying kinetics of the product. The drying characteristic curve corresponding to the dried product was obtained and the equation of drying rate was numerically established. Finally, diffusion coefficient and activation energy were estimated from the Arrhenius law and their values are respectively $(1.79 \times 10^{-8} < D_{eff} < 3.41 \times 10^{-8} \text{ m}^2/\text{s})$ and 10.81 kJ/kg.

REFERENCES

- [1] Koukouch, A., Bakhattar, I., Asbik, M., Idlimam, A., Zeghami, B., Aharoune, A. (2020). Analytical solution of coupled heat and mass transfer equations during convective drying of biomass: Experimental validation. *Heat and Mass Transfer*, 56: 1971-1983. <https://doi.org/10.1007/s00231-020-02817-w>

- [2] Bennini, M.A., Koukouch, A., Bakhattar, I., Asbik, M., Boushaki, T., Sarh, B., Elorf, A., Cagnon, B., Bonnamy, S. (2019). Characterization and combustion of olive pomace in a fixed bed boiler: Effects of particle sizes. *International Journal of Heat and Technology*, 37(1): 229-238. <https://doi.org/10.18280/ijht.370128>
- [3] Koukouch, A., Idlimam, A., Asbik, M., Sarh, B., Izrar, B., Bah, A., Ansari, O. (2015). Thermophysical characterization and mathematical modeling of convective solar drying of raw olive pomace. *Energy Conversion and Management*, 99: 221-230. <https://doi.org/10.1016/j.enconman.2015.04.044>
- [4] Bakhattar, I., Koukouch, A., Chater, H., Asbik, M., Mouaky, A., Idlimam, A. (2021). Thermodynamic analysis of batch adsorption isotherms of different types of olive pomace. *Heat and Mass Transfer*, 1-18. <https://doi.org/10.1007/s00231-021-03120-y>
- [5] Koukouch, A., Idlimam, A., Asbik, M., Sarh, B., Izrar, B., Bostyn, S., Bah, A., Ansari, O., Zegaoui, O., Amine, A. (2017). Experimental determination of the effective moisture diffusivity and activation energy during convective solar drying of olive pomace waste. *Renewable Energy*, 101: 565-574. <https://doi.org/10.1016/j.renene.2016.09.006>
- [6] Elorf, A., Bakhatar, I., Asbik, M., Sarh, B., Gillon, P. (2019). Fixed-bed biomass combustor: Air mass flow rate and particles size effects on ignition front propagation of solid olive waste. *Combustion Science and Technology*, 194(2): 365-377. <https://doi.org/10.1080/00102202.2019.1680070>
- [7] Harhar, H., Gharby, S., Guillaume, D., Charrouf, Z. (2010). Effect of argan kernel storage conditions on argan oil quality. *European Journal of Lipid Science and Technology*, 112(8): 915-920. <https://doi.org/10.1002/ejlt.200900269>
- [8] Guillaume, D., Charrouf, Z. (2011). Argan oil and other argan products: Use in dermocosmetology. *European Journal of Lipid Science and Technology*, 113(4): 403-408. <https://doi.org/10.1002/ejlt.201000417>
- [9] Moussaoui, H., Bahammou, Y., Idlimam, A., Lamharrar, A., Abdenouri, N. (2019). Investigation of hygroscopic equilibrium and modeling sorption isotherms of the argan products: A comparative study of leaves, pulps, and fruits. *Food and Bioproducts Processing*, 114: 12-22. <https://doi.org/10.1016/j.fbp.2018.11.002>
- [10] El Monfalouti, H., Guillaume, D., Denhez, C., Charrouf, Z. (2010). Therapeutic potential of argan oil: a review. *Journal of Pharmacy and Pharmacology*, 62(12): 1669-1675. <https://doi.org/10.1111/j.2042-7158.2010.01190.x>
- [11] Moussaoui, H., Bahammou, Y., Idlimam, A., Lamharrar, A., Abdenouri, N. (2019). Investigation of hygroscopic equilibrium and modeling sorption isotherms of the argan products: A comparative study of leaves, pulps, and fruits. *Food and Bioproducts Processing*, 114: 12-22. <https://doi.org/10.1016/j.fbp.2018.11.002>
- [12] Bejaoui, M., Taarji, N., Saito, M., Nakajima, M., Isoda, H. (2021). Argan (*Argania Spinosa*) press cake extract enhances cell proliferation and prevents oxidative stress and inflammation of human dermal papilla cells. *Journal of Dermatological Science*, 103(1): 33-40. <https://doi.org/10.1016/j.jdermsci.2021.06.003>
- [13] Charrouf, Z., Guillaume, D. (1999). Ethnoeconomical, ethnomedical, and phytochemical study of *Argania spinosa* (L.) Skeels. *Journal of Ethnopharmacology*, 67(1): 7-14. [https://doi.org/10.1016/S0378-8741\(98\)00228-1](https://doi.org/10.1016/S0378-8741(98)00228-1)
- [14] Hu, Y., Hamed, O., Salghi, R., Abidi, N., Jodeh, S., Hattb, R. (2017). Extraction and characterization of cellulose from agricultural waste argan press cake. *Cellul. Chem. Technol.*, 51: 263-272.
- [15] Afia, L., Salghi, R., Zarrouk, A., et al. (2012). Inhibitive action of argan press cake extract on the corrosion of steel in acidic media. *Portugaliae Electrochimica Acta*, 30(4): 267-279. <https://doi.org/10.4152/pea.201204267>
- [16] Moussaoui, H., Kouhila, M., Abdenouri, N., Bahammou, Y., Tagnamas, Z., Idlimam, A., Lamharrar, A. (2021). Experimental determination of the drying characteristics and the effective moisture diffusivity of the Dandelion leaves undergoing convective solar dryer. *Journal of Materials and Environmental Science*, 12(1): 153-160.
- [17] Motevali, A., Minaei, S., Banakar, A., Ghobadian, B., Khoshtaghaza, M.H. (2014). Comparison of energy parameters in various dryers. *Energy Conversion and Management*, 87: 711-725. <https://doi.org/10.1016/j.enconman.2014.07.012>
- [18] Prakash, O., Kumar, A. (2013). Historical review and recent trends in solar drying systems. *International Journal of Green Energy*, 10(7): 690-738. <https://doi.org/10.1080/15435075.2012.727113>
- [19] Moussaoui, H., Aghzzaf, A.A., Idlimam, A., Lamharrar, A. (2019). Modeling the solar drying of dandelion leaves by factorial experimental design. *Euro-Mediterranean Journal for Environmental Integration*, 4(1): 5. <https://doi.org/10.1007/s41207-018-0089-2>
- [20] Moussaoui, H., Idlimam, A., Lamharrar, A. (2018). The characterization and modeling kinetics for drying of taraxacum officinale leaves in a thin layer with a convective solar dryer. *International Conference on Electronic Engineering and Renewable Energy*, pp. 656-663. https://doi.org/10.1007/978-981-13-1405-6_75
- [21] Mohamed, L.A., Kouhila, M., Jamali, A., Lahsasni, S., Kechaou, N., Mahrouz, M. (2005). Single layer solar drying behaviour of Citrus aurantium leaves under forced convection. *Energy Conversion and Management*, 46(9-10): 1473-1483. <https://doi.org/10.1016/j.enconman.2004.08.001>
- [22] Mghazli, S., Ouhammou, M., Hidar, N., Lahnine, L., Idlimam, A., Mahrouz, M. (2017). Drying characteristics and kinetics solar drying of Moroccan rosemary leaves. *Renewable Energy*, 108: 303-310. <https://doi.org/10.1016/j.renene.2017.02.022>
- [23] Bahammou, Y., Moussaoui, H., Lamsayeh, H., et al. (2020). Water sorption isotherms and drying characteristics of rupturewort (*Herniaria hirsuta*) during a convective solar drying for a better conservation. *Solar Energy*, 201: 916-926. <https://doi.org/10.1016/j.solener.2020.03.071>
- [24] Van Meel, D.A. (1958). Adiabatic convection batch drying with recirculation of air. *Chemical Engineering Science*, 9(1): 36-44. [https://doi.org/10.1016/0009-2509\(58\)87005-0](https://doi.org/10.1016/0009-2509(58)87005-0)
- [25] Belghit, A., Kouhila, M., Boutaleb, B.C. (2000). Experimental study of drying kinetics by forced convection of aromatic plants. *Energy Conversion and Management*, 41(12): 1303-1321. [https://doi.org/10.1016/S0196-8904\(99\)00162-4](https://doi.org/10.1016/S0196-8904(99)00162-4)
- [26] Kaya, A., Aydın, O. (2009). An experimental study on drying kinetics of some herbal leaves. *Energy*

- Conversion and Management, 50(1): 118-124. <https://doi.org/10.1016/j.enconman.2008.08.024>
- [27] Doymaz, I. (2004). Drying kinetics of white mulberry. *Journal of Food Engineering*, 61(3): 341-346. [https://doi.org/https://doi.org/10.1016/S0260-8774\(03\)00138-9](https://doi.org/https://doi.org/10.1016/S0260-8774(03)00138-9)
- [28] Demirhan, E., Özbek, B. (2010). Drying kinetics and effective moisture diffusivity of purslane undergoing microwave heat treatment. *Korean Journal of Chemical Engineering*, 27(5): 1377-1383. <https://doi.org/10.1007/s11814-010-0251-2>
- [29] Kouhila, M., Moussaoui, H., Bahammou, Y., Tagnamas, Z., Lamsyehe, H., Lamharrar, A., Idlimam, A. (2020). Exploring drying kinetics and energy exergy performance of *Mytilus Chilensis* and *Dosidicus gigas* undergoing microwave treatment. *Heat and Mass Transfer*, 56(11): 2985-2999. <https://doi.org/10.1007/s00231-020-02909-7>
- [30] Moussaoui, H., Bahammou, Y., Tagnamas, Z., Kouhila, M., Lamharrar, A., Idlimam, A. (2021). Application of solar drying on the apple peels using an indirect hybrid solar-electrical forced convection dryer. *Renewable Energy*, 168: 131-140. <https://doi.org/10.1016/j.renene.2020.12.046>
- [31] Lemus-Mondaca, R., Vega-Gálvez, A., Moraga, N.O., Astudillo, S. (2015). Dehydration of *Stevia rebaudiana* Bertoni Leaves: Kinetics, Modeling and Energy Features. *Journal of Food Processing and Preservation*, 39(5): 508-520. <https://doi.org/10.1111/jfpp.12256>
- [32] Torki-Harchegani, M., Ghanbarian, D., Pirbalouti, A.G., Sadeghi, M. (2016). Dehydration behaviour, mathematical modelling, energy efficiency and essential oil yield of peppermint leaves undergoing microwave and hot air treatments. *Renewable and Sustainable Energy Reviews*, 58: 407-418. <https://doi.org/10.1016/j.rser.2015.12.078>
- [33] Wilkins, R., Brusey, J., Gaura, E. (2018). Modelling uncontrolled solar drying of mango waste. *Journal of Food Engineering*, 237: 44-51. <https://doi.org/10.1016/j.jfoodeng.2018.05.012>
- [34] Moussaoui, H., Lamsyehe, H., Idlimam, A., Lamharrar, A., Kouhila, M. (2018). Experimental study of the impact of drying parameters on dandelion root by a solar dryer. In *International Conference on Advanced Intelligent Systems for Sustainable Development*, pp. 12-20. https://doi.org/10.1007/978-3-030-12065-8_2
- [35] Ameri, B., Hanini, S., Benhamou, A., Chibane, D. (2018). Comparative approach to the performance of direct and indirect solar drying of sludge from sewage plants, experimental and theoretical evaluation. *Solar Energy*, 159: 722-732. <https://doi.org/10.1016/j.solener.2017.11.032>
- [36] Moussaoui, H., Lamsyehe, H., Idlimam, A., Lamharrar, A., Kouhila, M. (2019). Investigating the impact of drying parameters on the dandelion root using full factorial design of experiments. *International Journal of Sustainable Agricultural Management and Informatics*, 5(2-3): 83-96. <https://doi.org/10.1504/IJSAMI.2019.101666>
- [37] Benseddik, A., Azzi, A., Zidoune, M.N., Allaf, K. (2018). Mathematical empirical models of thin-layer airflow drying kinetics of pumpkin slice. *Engineering in Agriculture, Environment and Food*, 11(4): 220-231. <https://doi.org/10.1016/j.eaef.2018.07.003>
- [38] Beigi, M. (2016). Energy efficiency and moisture diffusivity of apple slices during convective drying. *Food Science and Technology*, 36: 145-150. <https://doi.org/10.1590/1678-457X.0068>
- [39] Doymaz, İ. (2012). Evaluation of some thin-layer drying models of persimmon slices (*Diospyros kaki* L.). *Energy Conversion and Management*, 56: 199-205. <https://doi.org/10.1016/j.enconman.2011.11.027>
- [40] Zhou, Y., Jin, Y. (2016). Mathematical modeling of thin-layer infrared drying of dewatered municipal sewage sludge (DWMSS). *Procedia Environmental Sciences*, 31: 758-766. <https://doi.org/10.1016/j.proenv.2016.02.066>
- [41] Kouhila, M., Moussaoui, H., Lamsyehe, H., Tagnamas, Z., Bahammou, Y., Idlimam, A., Lamharrar, A. (2020). Drying characteristics and kinetics solar drying of Mediterranean mussel (*mytilus galloprovincialis*) type under forced convection. *Renewable Energy*, 147: 833-844. <https://doi.org/10.1016/j.renene.2019.09.055>